Differential Functional Network Remodeling Induced by Low- and High-Frequency rTMS: Evidence From Concurrent fNIRS Monitoring

Hui Xie, Xin Li, Yan Wang, Gongcheng Xu, Yinghu Peng, Zhengsheng Hu, Zulin Dou, Zengyong Li, Qitao Tan, and Ming Zhang

***Abstract*— Repetitive transcranial magnetic stimulation (rTMS) at low-frequency (LF) and high-frequency (HF) has been shown to facilitate motor recovery after stroke, however the underlying neural network mechanism remains unclear. This study employed functional near-infrared spectroscopy (fNIRS) to monitor hemodynamic changes in real-time during rTMS, aiming to evaluate the immediate effects of LF- and HF-rTMS on functional network remodeling, and to explore the long-term impact of rTMS-induced neural changes on motor function recovery. A total of 108 stroke patients were randomly assigned to LF-rTMS, HF-rTMS or Sham groups and received 15-days of rTMS intervention. fNIRS was employed to detect hemodynamic changes during the intervention. The laterality index (LI) and the wavelet phase coherence (WPCO), based on wavelet transform, were used to describe functional network remodeling. Clinical scales were used to evaluate patients' behavioral outcomes. LF-rTMS significantly increased LI during the first intervention and induced WPCO changes between motor regions. In contrast, HF-rTMS produced delayed yet significant alterations in WPCO, with long-term intervention modulating both motor and cognitive networks. After 15 days, both LF- and HF-rTMS showed significant behavioral improvements correlated with WPCO changes. The rTMS-fNIRS approach provided neural mechanistic evidence for the role of rTMS in promoting functional recovery. LF-rTMS mitigates abnormal interhemispheric inhibition and induces behavioral improvements during the short-term treatment process. In contrast, HF-rTMS requires sustained stimulation to achieve remodeling effects but may offer broader rehabilitative benefits. These behavioral changes result from acute neural modulation induced by rTMS, which may consolidate transient plasticity into long-term motor recovery through repeated interventions.**

***Index Terms*— Transcranial magnetic stimulation (TMS), functional near-infrared spectroscopy (fNIRS), motor dysfunction after stroke, functional network remodeling.**

Received 10 June 2025; revised 13 August 2025; accepted 5 September 2025. Date of publication 18 September 2025; date of current version 29 September 2025. This work was supported in part by the National Key Research and Development Program of China under Grant 2023YFC3603703, in part by the National Natural Science Foundation of China under Grant 32271370 and Grant 12302421, and in part by Hong Kong Polytechnic University Internal Research Fund: Start-Up Fund for RAPs under the Strategic Hiring Scheme under Grant P0046559. *(Corresponding authors: Qitao Tan; Ming Zhang.)*

This work involved human subjects or animals in its research. Approval of all ethical and experimental procedures and protocols was granted by the Human Ethics Committee of the Third Affiliated Hospital, Sun Yat-sen University under Application No. [2021]02-333-01.

Hui Xie, Yan Wang, Qitao Tan, and Ming Zhang are with the Department of Biomedical Engineering, Faculty of Engineering, and the Research Institute for Sports Science and Technology, The Hong Kong Polytechnic University, Hong Kong, SAR, China (e-mail: qitao.tan@polyu.edu.hk; ming.zhang@polyu.edu.hk).

Xin Li and Zulin Dou are with the Department of Rehabilitation Medicine, The Third Affiliated Hospital, Sun Yat-sen University, Guangzhou 510630, China.

Gongcheng Xu and Zhengsheng Hu are with the Department of Biomedical Engineering, Faculty of Engineering, The Hong Kong Polytechnic University, Hong Kong, SAR, China.

Yinghu Peng is with the CAS Key Laboratory of Human-Machine Intelligence-Synergy Systems, Shenzhen Institutes of Advanced Technology (SIAT), Chinese Academy of Sciences (CAS), Shenzhen 518055, China.

Zengyong Li is with Beijing Key Laboratory of Rehabilitation Technical Aids for Old-Age Disability, National Research Center for Rehabilitation Technical Aids, Beijing 100176, China.

Digital Object Identifier 10.1109/TNSRE.2025.3611796

I. Introduction

STROKE is a major cause of mortality and long-term disability worldwide [1], often resulting in extensive neuronal loss in localized brain regions and subsequent motor control deficits. Following a stroke, functional connectivity in the brain becomes disrupted, with more than 80% of survivors experiencing varying degrees of motor impairment. Among these, one-third suffer from permanent functional deficits [2], [3], severely limiting their ability to reintegrate into society and return to work, thus underscoring the urgent need for precision rehabilitation.

Modern rehabilitation research suggests that upper-limb motor function recovery after stroke largely depends on neuroplasticity [4], which may occur spontaneously or be augmented through neuromodulatory interventions such as repetitive transcranial magnetic stimulation (rTMS) [5], [6]. rTMS induced cortical currents via low-frequency (LF) or high-frequency (HF) magnetic pulses, which respectively inhibit or excite neuronal activity, achieving a rebalancing of local neural activity [7]. Although the clinical efficacy of rTMS in improving motor function post-stroke has been demonstrated [8], the neural mechanisms underlying LF- and HF-rTMS remain unclear,

creating uncertainty in clinical application. Neuroplasticity-driven remodeling of brain networks is considered pivotal for motor function recovery [9], [10], as it allows examination of coordinated interactions among multiple brain regions and provides a holistic perspective on brain activity [5]. This approach elucidates the integration and processing of information across the whole brain, thereby offering insights into global brain dynamics beyond isolated regional activity [11]. Therefore, further investigation is required to determine how LF- and HF-rTMS influence these processes.

In recent years, combining rTMS with neuroimaging has become an important research focus [12], [13]. Neuroimaging enables the direct visualization of cortical activity changes, providing new insights into how rTMS facilitates motor network remodeling [14], [15]. A major challenge in this area is achieving effective dynamic monitoring of the rTMS intervention process. Functional near-infrared spectroscopy (fNIRS) is particularly well-suited for this purpose [16]. By continuously monitoring cortical hemodynamic changes and neurovascular coupling during rehabilitation, fNIRS provides insights into neural activity dynamics [17], [18]. As a result, fNIRS has attracted growing interest in clinical research.

Compared with other functional imaging techniques, the integration of rTMS and fNIRS (rTMS-fNIRS) provides a higher signal-to-noise ratio, moderate spatiotemporal resolution, and non-radiative properties than rTMS combined with functional magnetic resonance imaging (fMRI) [19] or electroencephalography (EEG) [20], while also demonstrating strong resistance to motion artifacts [21]. More importantly, the hemodynamic responses driven by neural metabolic demand, as measured by rTMS-fNIRS, exhibit a high degree of consistency with fMRI results [22], while remaining unaffected by electromagnetic interference. Given these advantages, rTMS-fNIRS provides an ideal approach for investigating the dynamic effects of excitatory and inhibitory stimulation on functional network remodeling.

Despite these methodological strengths, clinical evidence for rTMS-fNIRS in stroke populations remains limited [21]. Existing studies are predominantly small-sample feasibility or exploratory investigations [23], indicating that this technique can capture cortical hemodynamic responses to excitatory and inhibitory stimulation at the bedside in real time [24], [25]. However, large-scale, longitudinal, multicenter trials remain scarce, partly due to challenges such as hardware compatibility, artifact suppression, and the lack of standardized protocol [5]. In our preliminary work, we established a robust concurrent rTMS-fNIRS acquisition and processing framework capable of continuously tracking time-varying changes in brain networks and validating rapid neuroplastic signatures during stimulation, thereby providing a solid technical and theoretical foundation for the present study.

In summary, this study conducts a longitudinal clinical trial using rTMS-fNIRS to investigate both the immediate effects of LF- and HF-rTMS on functional network remodeling and the long-term impact of rTMS-induced neural changes on motor recovery in stroke patients. Based on previous studies, we hypothesize that LF- and HF-rTMS induce distinct remodeling patterns that may have differential effects on behavioral outcomes. This study will expand our understanding of the neural mechanisms underlying rTMS-induced improvements in motor function. The findings will provide theoretical guidance for the clinical selection of rTMS protocols and offer scientific evidence to support individualized and precision rehabilitation strategies.

II. Methods

A. Participants

This study is a double-anonymous, randomized, three-arm follow-up trial. A total of 108 right-handed adults with stroke (aged 40-80 years) in the subacute stage and in stable condition were recruited for the rTMS-fNIRS program. The inclusion criteria were: (1) first-ever stroke confirmed by fMRI or cranial computed tomography; (2) subacute stage was defined as 7 days to 6 months post-onset; (3) presence of mild to severe unilateral motor dysfunction; and (4) with Mini-Mental State Examination scores ≥24, indicating no significant cognitive impairment. Participants were excluded from the study if they had: (1) prior history of stroke, traumatic brain injury, or brain tumor; (2) severe cardiac, pulmonary, hepatic, or renal disease; (3) history or family history of epilepsy; (4) presence of metallic implants such as pacemakers, cranial metal; (5) new infarcts or secondary hemorrhages; and (6) severe cervical spine pathology. All participants were informed of the study's purpose, procedures, schedule, and relevant precautions. Each enrolled participant signed a written informed consent. The experimental procedures were approved by the Human Ethics Committee of the Third Affiliated Hospital, Sun Yat-sen University ([2021]02-333-01). It has been registered with the Chinese Clinical Trials Registry website under the trial number ChiCTR2100054527.

B. Study Design and Randomization

Participants were randomly assigned to one of three groups: LF-rTMS, HF-rTMS, or Sham group, and received 15-days continuous rTMS intervention. The LF-rTMS group received 1 Hz, 600 s, total of 600 pulses of intervention on the primary motor area (M1) of the contralesional hemisphere. The HF-rTMS group received 5 Hz, 2 s, intertrain interval 4 s, 100 trains, total of 1000 pulses intervention on ipsilesional hemisphere M1. The Sham group followed the HF-rTMS protocol, but the coil was oriented 90° away from the target site and positioned 5 cm from the scalp, producing only auditory and somatosensory cues without effective stimulation. This setup mimicked somatosensory sensations without exerting substantial neural effects [26], [27]. The above protocol complies with the rTMS guidelines for clinical and research applications [28]. All patients received conventional stroke treatment, including common physical therapy and occupational therapy.

Neurophysiological and behavioral assessments were performed on days 1 and 15 of the intervention. All evaluations were conducted in a quiet treatment room. Before measurement began, all participants were asked to sit still for 10-20 min to reduce hemodynamic variability due to prior activity. fNIRS was then used to continuously monitor dynamic hemodynamic signals during 10 min resting and

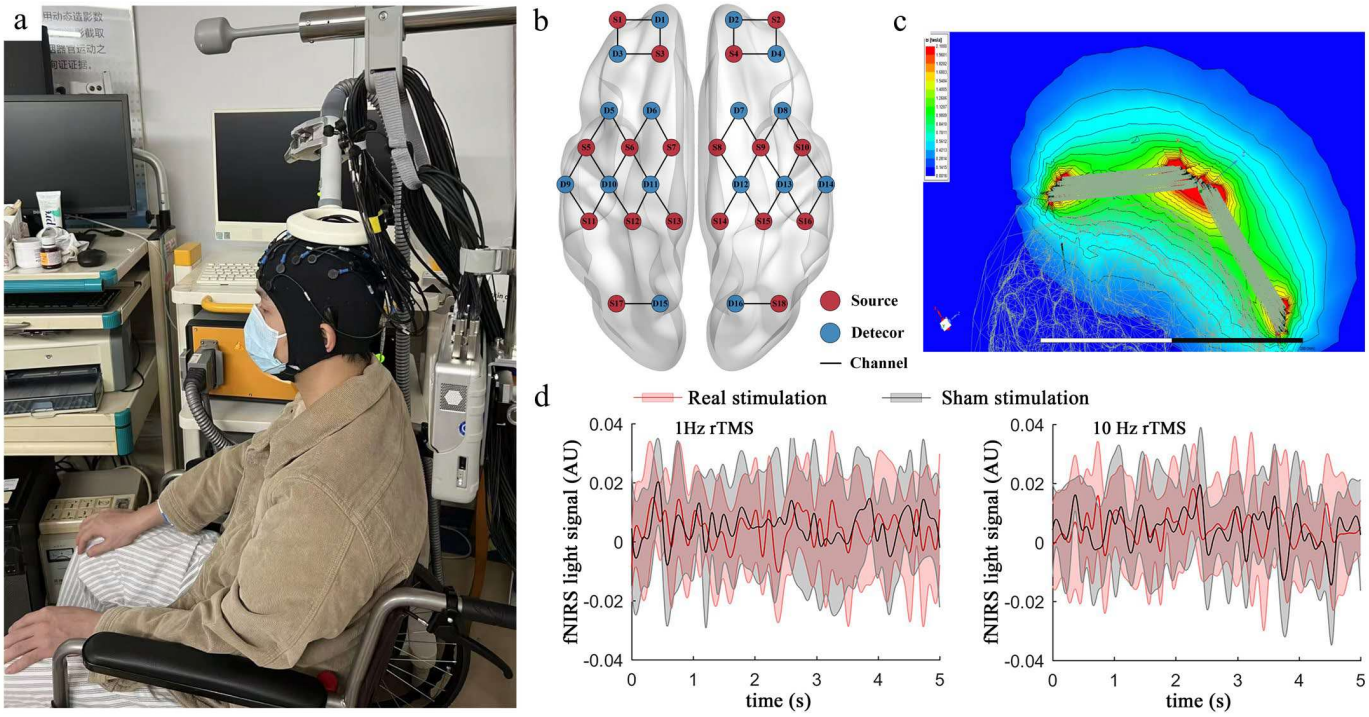

Fig. 1. Experimental design and preparation. (a) rTMS-fNIRS integration and clinical application. (b) fNIRS probe set. (c) Simulation of magnetic field intensity attenuation. (d) Magnetic field effect check.

rTMS intervention state. Participants remained seated, relaxed, and were instructed to avoid movement or speech. Upper-limb motor function was assessed using standardized clinical scales, including the Fugl-Meyer Assessment (FMA), National Institutes of Health Stroke Scale (NIHSS), Modified Barthel Index (MBI), Modified Rankin Scale (mRS), and Action Research Arm Test (ARAT).

One day before the experiment, a rehabilitation therapist collected participants' demographic data and completed the initial clinical assessments. Using MATLAB, participants were randomly assigned numbers 1 to 108 and allocated to LF-rTMS, HF-rTMS, or Sham groups based on enrollment sequence. Blinding was maintained throughout the study. The therapist administering rTMS was aware of the stimulation parameters but was not involved in assessment or data analysis. Statistical analysts were also blinded to group assignments and not involved in the randomization process.

C. Integration of rTMS-fNIRS

The rTMS device (NS1000, Yiruide, Wuhan, China) was positioned above a dual-wavelength (740 nm and 850 nm) multi-channel continuous-wave near-infrared tissue oxygenation monitoring system (NirSmart, Danyang Huichuang Medical Equipment Co., Beijing, China) [29] (Fig. 1 a). A 120° figure-eight coil was used to ensure adequate stimulation depth while allowing simultaneous signal acquisition. fNIRS optodes were symmetrically arranged over both hemispheres according to the international 10-20 EEG system. The calibration function of the instrument and corresponding template were used to fit the channels according to different head sizes of the participants. To ensure the placement of the probes as accurate as possible, we utilized an elastic cap and fixed hard rubber to maintain consistent electrode spacing for each participant. The source-detector distance was maintained at 30 mm. The clasps and springs were used to secure the optode template to the scalp, ensuring firm and direct contact between the light sources, detectors, and the participant's skin.

A total of 18 light sources and 16 detectors were arranged to form 38 channels covering both the ipsilesional and contralesional hemispheres. The targeted cortical regions included the prefrontal cortex (iPFC/cPFC), dorsolateral prefrontal cortex (iDLPFC/cDLPFC), superior frontal cortex (iSFC/cSFC), premotor and primary motor cortex (iMC/cMC), primary somatosensory cortex (iS1/cS1), and occipital cortex (iOC/cOC) (Fig. 1 b). Direct physical contact between the rTMS and fNIRS devices was avoided. We initially set all differential path-length factors to 7.0, and the sampling frequency was set at 10 Hz.

To ensure effective magnetic field intensity of rTMS, the degree of magnetic field attenuation was simulated using ANSYS based on the actual position information of the coil (Fig. 1 c). In addition, by comparing the fNIRS signals under the real 1 Hz, 10 Hz, and Sham stimulation conditions, no significant differences were observed; therefore, the influence of the rTMS magnetic field on fNIRS measurements was excluded (Fig. 1 d). At the beginning of the experiment, the resting motor threshold (rMT) was determined to calibrate stimulation intensity. The initial stimulation intensity was set at 30% of the maximum output of the device. The rMT was defined as the minimum intensity required to elicit motor-evoked potentials greater than 50 μV in at least 10 of 20 consecutive trials in the abductor pollicis brevis muscle [30]. For all participants, the stimulation intensity during the

intervention was then adjusted to 100% of the rMT. In cases where rMT could not be elicited from the iM1, the homologous cortical region in the contralesional hemisphere was designated as the target measurement site.

D. Data Preprocessing

Detailed methods for preprocessing fNIRS data have been described in our previous studies [31], [32], [33], [34]. The modified Beer–Lambert law was applied to convert optical density signals into changes in oxyhemoglobin concentration ($\Delta[HbO_2]$), which has been shown to be highly sensitive for characterizing information processing in cortical regions [35]. A sliding average method and a zero-phase fifth-order Butterworth band-pass filter were applied to extract signals within 0.005-2 Hz, eliminating ultra-low-frequency components (below 0.005 Hz) from the raw data. Given that participants may inevitably exhibit movements or produce unconscious speech during the experiment, the temporal derivative distribution repair algorithm [36], [37] was applied to the $\Delta[HbO_2]$ signals to correct motion artifacts. Residual spike-like artifacts were further reduced using a sliding average method and cubic spline interpolation. To address shallow-layer hemodynamic interference, a common average reference (CAR) spatial filtering approach [38], [39] was applied by calculating the mean signal across all channels and subtracting it from each channel at each time point [40]. Subsequently, independent component analysis (ICA) and principal component analysis (PCA) were utilized to separate scalp blood pressure fluctuations, skin blood flow interference, and non-evoked hemodynamic components [41], [42]. All derived components were subjected to visual inspection to identify those associated with noise and artifacts, including cardiac pulsation and respiratory signals, thereby reducing interference in fNIRS signal analysis and improving the signal-to-noise ratio. Finally, wavelet transform using complex Morlet wavelets was applied to identify and retain oscillatory signals in the 0.01-0.08 Hz, corresponding to the hemodynamic response of neural activity [43].

E. Functional Network Remodeling Index

The wavelet transform results were averaged in the time domain to obtain the wavelet amplitude of the fNIRS signal at each time and frequency. This amplitude reflects the magnitude of regional cerebral blood flow fluctuations induced by cortical activity at a given frequency and is calculated over the entire rTMS intervention period rather than from isolated epochs. This parameter provides a quantitative measure of task-related hemodynamic activation in the cerebral cortex. The amplitude is further used to calculate the laterality index (LI) for a given pair of ipsilesional and contralesional homologous regions, according to the following formula:

$$LI = \frac{\sum ÆA_{contralesional} - \sum ÆA_{\text{ipsilesional}}}{\sum ÆA_{contralesional} + \sum ÆA_{\text{ipsilesional}}} \quad (1)$$

where $A_{contralesional}$ and $A_{\text{ipsilesional}}$ represent the activation in the contralesional and ipsilesional hemispheres, respectively. LI values range from 1 (exclusive contralesional activation) to −1 (exclusive ipsilesional activation), with values near zero indicating hemispheric balance. Physiologically, LI reflects the degree of interhemispheric asymmetry in activation.

In addition to the LI, functional connectivity serves as another key indicator in this study for evaluating brain network remodeling. Some researchers have already applied this approach in medical studies to analyze relationships betweenvarious physiological signals [44], [45]. In this study, functional connectivity is quantified using wavelet phase coherence (WPCO), which evaluates the correlation between two signals based on the consistency of their instantaneous phases [46]. WPCO is likewise computed from the time series over the entire rTMS intervention period, enabling continuous tracking of connectivity changes throughout stimulation. Using wavelet transform, the instantaneous phases of the wavelet signals from two regions at frequency f are extracted, and the phase difference $\Delta\phi_1(f, t_n)$ is obtained by subtracting one phase from the other at each time point t_n. This measure quantifies the instantaneous phase consistency between two signals over a continuous time series, enabling the analysis of potential functional connectivity across different time series within a specific frequency [47], [48]. WPCO is defined as:

$$\text{WPCO}(f) = \sqrt{\langle\cos\Delta\phi(f)\rangle^2 + \langle\sin\Delta\phi(f)\rangle^2}, \quad f \in 0.01 - 0.08 \quad (2)$$

WPCO values range from 0 (no phase consistency) to 1 (perfect phase locking), with higher values indicating stronger functional connectivity between the two regions at the given frequency. Physiologically, higher WPCO reflects more stable temporal coordination between cortical areas, suggesting enhanced network integration. To eliminate confounding effects of spurious significance in WPCO, the amplitude-adaptive Fourier transform method was employed to enhance the identification of functional connectivity strength.

F. Statistical Analysis

The Kolmogorov-Smirnov test and Levene's test were used at the group level to assess the normality of variance and the homogeneity of data outcomes.

One-way ANOVA was conducted for inter-group analysis, primarily examining significant differences in demographic characteristics baseline, as well as region-wise LI, WPCO and behavioral changes among the Sham, LF-rTMS, and HF-rTMS groups. For multiple comparisons between groups, Bonferroni correction was applied, setting the significance threshold at $p < 0.0167$ (0.05/3). Independent-sample t-tests and Pearson correlation analysis were used for intra-group analysis, primarily to assess significant pre-to-post intervention changes in behavioral and functional network remodeling index, as well as to identify potential correlations between these changes.

III. Results

A. Demographic Characteristic

During the study period, a total of 192 stroke patients were hospitalized for rehabilitation treatment. Among them, 36 did not meet the inclusion criteria, 22 were excluded, and

TABLE I
DEMOGRAPHIC AND CLINICAL EVALUATION BASELINE: MEAN ± SD

Characteristics	Sham	LF-rTMS	HF-rTMS	p-value
Sample size (n)	34	26	34	/
Age (years)	58.57 ± 7.63	59.22 ± 9.76	60.01 ± 12.12	0.674
Gender (n)				
Male / Female	25 / 9	14 / 12	20 / 14	0.247
Type of stroke (n)				
Infarction / Hemorrhage	22 / 12	21 / 5	22 / 12	0.192
Ipsilesional hemisphere (n)				
Right / Left	16 / 18	16 / 10	15 / 19	0.373
Post-onset duration (days)	54.86 ± 40.10	65.92 ± 46.69	52.66 ± 35.68	0.390
Behavioral measures				
MMSE	24.61 ± 4.73	24.33 ± 5.94	24.12 ± 5.47	0.925
FMA	22.00 ± 17.24	21.62 ± 16.27	23.01 ± 19.79	0.952
NIHSS	5.67 ± 2.39	6.22 ± 1.96	5.56 ± 2.81	0.638
MBI	55.70 ± 24.67	61.44 ± 20.73	54.91 ± 25.92	0.626
ARAT	8.97 ± 15.32	6.22 ± 13.29	9.95 ± 15.98	0.686
mRS	3.61 ± 0.71	3.50 ± 0.62	3.56 ± 0.88	0.895

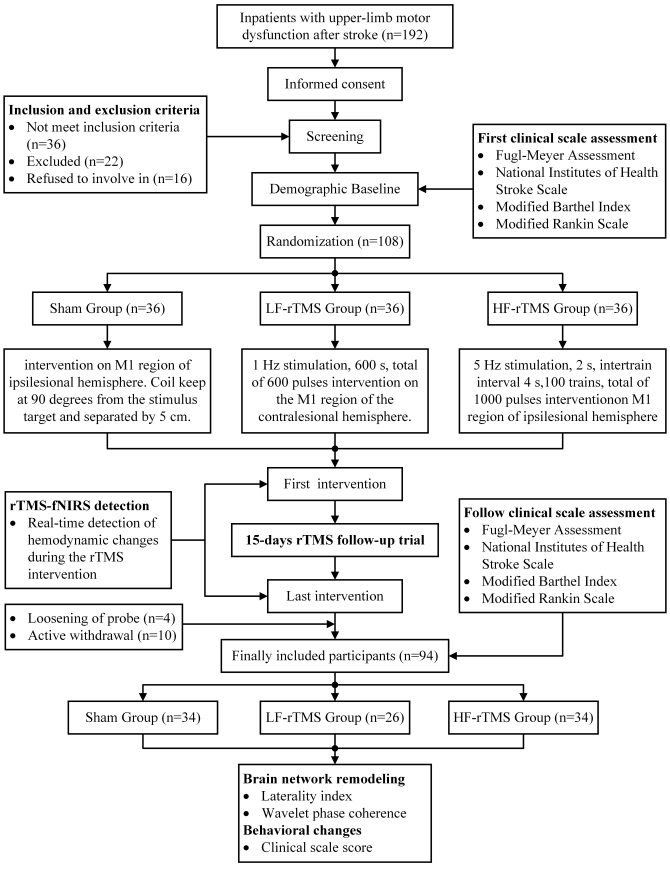

Fig. 2. Study flow chart. LF: Low-frequency, HF: High-frequency, rTMS: repetitive transcranial magnetic stimulation.

16 refused to involve. The remaining 108 participants were randomly assigned to three groups and completed the initial rTMS intervention and assessment. The detailed enrollment process is shown in Fig. 2.

During the experiment, 4 participants were excluded from the final analysis due to probe loosening, and 10 participants due to active withdrawal were excluded from the final analysis. The remaining 94 participants completed the 15-days follow-up trial and were included in the statistical analysis, including Sham (n = 34), LF-rTMS (n = 26), and HF-rTMS (n = 34). No significant differences were observed among the three groups in terms of demographic characteristics or baseline clinical evaluations, as shown in Table I.

B. rTMS Induced Brain Functional Network Remodeling Changes During Intervention

The lateralization results obtained from rTMS-fNIRS assessments are shown in Fig. 3. During the first intervention, compared to the Sham group, LF-rTMS significantly increased LI values between bilateral SFC (p = 0.034), MC (p = 0.017), and S1 (p = 0.012) (Fig. 3 a-c), while there was no significant difference between Sham and HF-rTMS. After 15 days intervention, HF-rTMS significantly decreased LI values between bilateral SFC (p = 0.028) (Fig. 3 d). There was no significant difference between Sham and LF-rTMS.

The functional connectivity results are shown in Fig. 4. The visualization highlights the distribution of brain network remodeling changes. During the first intervention, LF-rTMS stimulation led to a significant decrease in WPCO values compared to the sham group in the following regions: cDLPFC-iMC (p = 0.045), cSFC-cOC (p = 0.042), cSFC-iSFC (p = 0.034), cSFC-iMC (p = 0.038), cMC-cS1 (p = 0.007), cMC-iOC (p = 0.046), cMC-iMC (p = 0.006), cMC-iS1 (p = 0.018), cMC-iOC (p = 0.029), cS1-iS1 (p = 0.029), iSFC-cMC (p = 0.013), iMC-cS1 (p = 0.025) (Fig. 4a). After 15-days of intervention, compared to the Sham group, LF-rTMS showed a significant decrease in WPCO values between cPFC-cSFC (p = 0.042), cDLPFC-cSFC (p = 0.038), cDLPFC-cMC (p = 0.031), and cSFC-iSFC (p = 0.037) (Fig. 4 b). In addition, HF-rTMS showed a significant decrease decrease of WPCO values between the following regions: cPFC-cSFC (p = 0.004), cDLPFC-cSFC (p = 0.032), cPFC-iSFC (p = 0.004), cPFC-iMC (p = 0.035), cPFC-iS1 (p = 0.016), cDLPFC-iSFC (p = 0.05), cDLPFC-cMC (p = 0.031), cSFC-iSFC (p < 0.001), iDLPFC-cSFC (p = 0.047), iSFC-

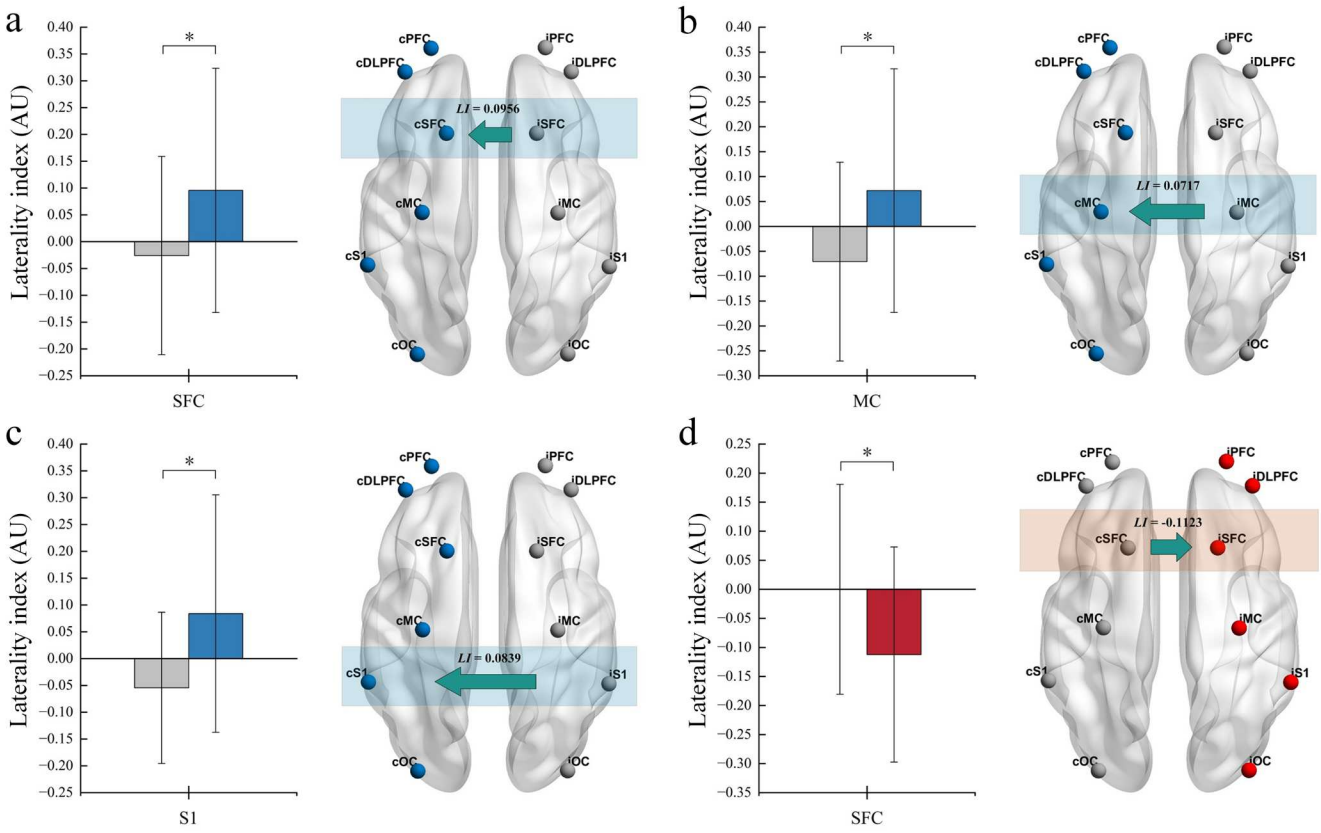

Fig. 3. The significant changes in laterality indices of each brain region between the Sham and rTMS group.

TABLE II
COMPARISON RESULTS OF BEHAVIORAL CHANGES IN RTMS PERIOD: MEAN ± SD

Behavioral change	Group			*p*-value
	Sham	LF-rTMS	HF-rTMS	(*a* / *b*)
FMA	2.71 ± 3.79	6.81 ± 8.22	4.65 ± 4.45	0.006* / 0.154
NIHSS	-0.64 ± 0.99	-1.27 ± 0.87	-1.29 ± 0.76	0.007* / 0.003*
MBI	4.91 ± 7.93	8.06 ± 7.63	8.73 ± 8.44	0.195 / 0.058
ARAT	2.27 ± 7.68	3.38 ± 5.37	2.27 ± 3.70	0.547 / 0.997
mRS	-0.27 ± 0.45	-0.47 ± 0.51	-0.36 ± 0.55	0.193 / 0.467

Abbreviations: "a" represents the statistical difference of Sham vs. LF-rTMS, and "b" represents the statistical difference of Sham vs. HF-rTMS. "*" indicate *p*-value < 0.05.

cMC (p = 0.021), iSFC-cS1 (p = 0.024) and iSFC-iM1 (p = 0.021) (Fig. 4 c).

C. rTMS Induced Behavioral Changes After Long-Term Intervention

The behavioral changes after 15 consecutive days of intervention in the three groups are shown in Table II. Both LF- and HF-rTMS showed significant changes in the behavioral assessment compared with the Sham group. Specifically, the significant changes in patients of the LF-rTMS group originated from FMA (p = 0.006) and NIHSS (p = 0.007), while patients of the HF-rTMS group only showed significant improvement in NIHSS (p = 0.003).

The correlation analysis results of behavioral and brain functional network remodeling indicators changes are shown in Fig. 5. The results of FMA indicated that behavioral changes were significantly negatively correlated with WPCO values changes of iMC-cOC (r = −0.383, p = 0.027) and iS1-cOC (r = −0.371, p = 0.009) in LF-rTMS group (Fig. 5 a). However, there was no significant correlation with HF-rTMS.

NIHSS had a broader correlation with the neural remodeling induced by rTMS. NIHSS scores changes were significantly positively correlated with WPCO changes of LF-rTMS in the following connectivity (Fig. 5 b): cMC-iOC (r = 0.453, p = 0.017), iPFC-cMC (r = 0.409, p = 0.029), iPFC-iMC (r = 0.459, p = 0.016), iMC-cOC (r = 0.368, p = 0.046), iMC-iOC (r = 0.384, p = 0.039), and iS1-cOC (r = 0.392, p = 0.036). Moreover, the NIHSS scores change were significantly positively correlated with WPCO changes of HF-rTMS in the following connectivity (Fig. 5 c): cPFC-cSFC (r = 0.336, p = 0.043), cPFC-iSFC (r = 0.531, p = 0.002), cPFC-iMC (r = 0.362, p = 0.032), cDLPFC-cSFC (r = 0.349, p = 0.037), cDLPFC-iSFC (r = 0.393, p = 0.021), and iPFC-cSFC (r = 0.463, p = 0.008).

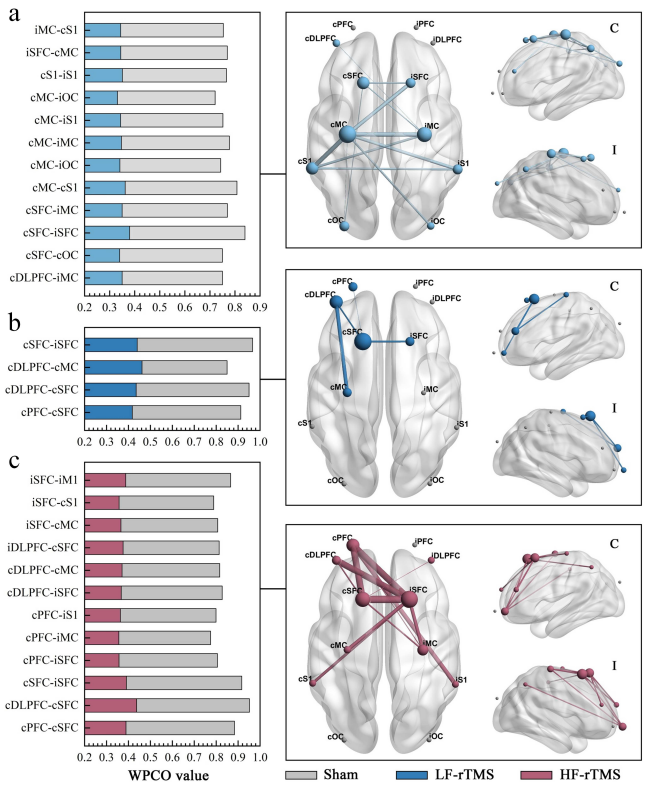

Fig. 4. The intergroup significant differences in functional connectivity and visual map. The connectivity line indicates significant differences in WPCO values between the two regions. Line thickness indicates the significance degree. Cool colors represent LF-rTMS, and warm colors represent HF-rTMS. "C", Contralesional hemisphere. "I", ipsilesional hemisphere.

IV. Discussion

This study investigated the immediate effects of LF- and HF-rTMS on brain functional network remodeling and the long-term behavioral benefits associated with these neuroplastic changes. The results indicated that LF-rTMS induced more favorable early-stage functional network remodeling, while the effects of HF-rTMS became progressively evident over the course of the intervention. In terms of behavioral outcomes, 15-days LF-rTMS intervention led to greater improvements in motor function among patients with motor deficits. These findings provide insights into the mechanisms by which rTMS facilitates functional recovery through modulation of brain networks.

A. Immediate Effects of LF- and HF-rTMS

In this study, we employed an integrated rTMS-fNIRS approach to monitor real-time changes in functional network remodeling on the first and fifteenth days of intervention, providing insights into immediate neuroregulatory effects. The lateralization results showed that LF-rTMS significantly shifted cerebral blood flow toward the contralesional hemisphere in the SFC, MC, and S1 regions. This phenomenon may be attributed to LF-rTMS activating inhibitory neurons [24], which increases the demand for blood and nutrients supply in the stimulated region [49]. The 1 Hz stimulation frequency of LF-rTMS corresponds to the firing rate of inhibitory interneurons; sustained stimulation enhances their activity, thereby reducing cortical excitability and stabilizing the stimulated region [50]. As a result, LF-rTMS may suppress excessive interhemispheric inhibition from the contralesional to the ipsilesional hemisphere, thereby restoring interhemispheric balance and promoting motor recovery.

Furthermore, we found that LF-rTMS rapidly induced changes in functional connectivity within the affected cortical regions and related networks during the early phase of the intervention, demonstrating a clear remodeling effect. This finding is consistent with previous research [51], [52]. In contrast, HF-rTMS showed less significant functional network remodeling at the early stage; however, its effects became more pronounced by day 15, suggesting a cumulative mechanism underlying its neuromodulatory action. These observations imply that HF-rTMS may require repeated stimulation to produce substantial functional network changes and enhance.

Our analysis of functional networks revealed that both LF- and HF-rTMS modulate key motor-related nodes, including bilateral SFC and MC. Such dynamic remodeling of motor regions supports the brain's adaptive and compensatory mechanisms for functional recovery [53], [54]. Additionally, HF-rTMS was observed to influence networks involving cPFC and cDLPFC. While these regions are not classically considered motor-related, they may enhance cognitive control over motor execution [55], [56]. Indeed, the capacity of stroke patients to learn and retain motor patterns may depend on the engagement of these regions [57].Taken together, these findings suggest that LF- and HF-rTMS engage different mechanisms of network remodeling, which play an important role in the rehabilitation of motor function after stroke [58], [59]. Specifically, LF-rTMS primarily exerts an inhibitory effect, which can alleviate abnormal interhemispheric inhibition and lead to direct behavioral improvements during short-term treatment. In contrast, HF-rTMS requires a longer duration of cumulative stimulation to achieve remodeling, but it may provide broader rehabilitative benefits, such as improving motor planning abilities in patients.

B. Long-Term Effects of LF- and HF-rTMS

After 15 days of intervention, behavioral assessments showed significant improvements in motor function in both the LF- and HF-rTMS groups, consistent with findings from other clinical studies [60]. However, in the present study, LF-rTMS produced superior behavioral outcomes compared to HF-rTMS. While this finding is supported by certain studies [61], other meta-analyses have reported contradictory results [62]. The non-significant behavioral outcomes observed in the HF-rTMS group may be due to its underlying mechanism of action; as previously noted, the effects of HF-rTMS require time to accumulate. Therefore, a longer-term follow-up study is warranted to confirm these findings.

Previous studies have demonstrated that rTMS intervention can upregulate the expression of brain-derived neurotrophic factor, thereby promoting neurogenesis and synaptic plasticity and providing a biological foundation for long-term functional recovery [63], [64]. Our correlation analyses revealed that

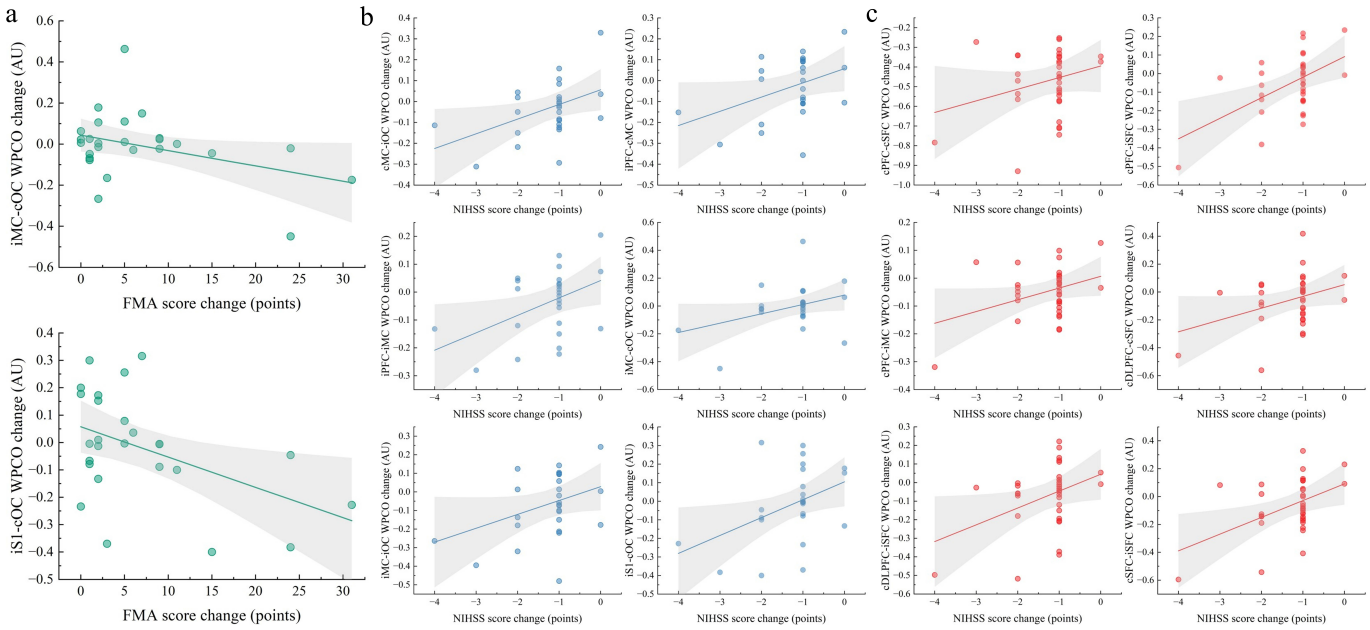

Fig. 5. Results of correlation between behavioral and neural remodeling changes. (a) The significant correlation results between FMA and LF-rTMS. (b-c) More detailed correlation results between NIHSS and LF-rTMS, as well as HF-rTMS.

behavioral changes in the LF-rTMS group were primarily associated with remodeling in bilateral MC-related networks, whereas improvements in the HF-rTMS group were mainly linked to changes in the cPFC, cDLPFC, and bilateral SFC networks. These remodeling effects originated from immediate neural stimulation induced by rTMS, suggesting that repeated sessions can accumulate and translate short-term remodeling into sustained behavioral improvements.

Such long-term improvements may involve multilayered neuroadaptive processes, with hemodynamic changes observed via fNIRS providing supporting evidence. By modulating local cerebral blood flow and neural activity, rTMS directly promotes functional recovery in damaged regions. These local changes may further enhance or restore functional connectivity, ultimately improving coordination within the entire motor network. With repeated interventions, short-term neuroplastic effects can be consolidated and maintained, leading to stable improvements in motor function.

This study has several limitations. First, due to the current immaturity of short-separation channel techniques and the challenges associated with their widespread implementation in large-scale clinical data collection, short-channel measurements were not employed in this study. To address scalp hemodynamic oscillations during rTMS, we employed a preprocessing strategy combining CAR spatial filtering, PCA, and ICA to remove artifacts related to scalp blood pressure, skin blood flow, and non–task-related hemodynamic components [65]. This approach allowed for a more accurate isolation of cortical hemodynamic responses [66]. In future studies, we aim to gradually refine and standardize short-channel methodologies, incorporating them as a routine component of the experimental protocol. Second, the observation window in this study was limited to 15 days, which may not fully capture the cumulative effects of rTMS. This constraint is particularly relevant for HF-rTMS, as its neuromodulatory impact on brain network remodeling may evolve more gradually and manifest beyond the two-week period. Consequently, the present findings may underestimate the full therapeutic potential of HF stimulation. Future studies will incorporate extended follow-up periods and additional intermediate assessments to better delineate the temporal trajectory and cumulative impact of rTMS-induced network changes. Third, to minimize participant burden during concurrent rTMS–fNIRS sessions and reduce motion-related artifacts, we limited behavioral endpoints to validated clinical scales. Future work will integrate low-burden quantitative measures to further enrich behavioral assessment. Finally, this study focused on patients in the subacute phase of stroke without stratification by lesion side, which may influence the neuromodulatory effects of rTMS and narrow the generalizability of the findings. Future work will incorporate these variables to better elucidate individualized stimulation responses.

V. Conclusion

This study indicates that although both LF- and HF-rTMS improve upper-limb motor function in stroke patients, they involve different mechanisms of brain functional network remodeling. LF-rTMS can alleviate abnormal interhemispheric inhibition and promote the recovery of motor function within a short period. However, HF-rTMS requires continuous stimulation to produce a remodeling effect, which may bring broader rehabilitation benefits, such as the improvement of motor planning ability. Further analysis indicates that behavioral improvements are closely associated with long-term alterations in functional brain networks induced by rTMS, and these neuroplastic changes result from the cumulative effects of repeated stimulation.

REFERENCES

[1] S. Mendis, "Stroke disability and rehabilitation of stroke: World health organization perspective," *Int. J. Stroke*, vol. 8, no. 1, pp. 3–4, Jan. 2013.

[2] G. Morone, I. Cocchi, S. Paolucci, and M. Iosa, "Robot-assisted therapy for arm recovery for stroke patients: State of the art and clinical implication," *Expert Rev. Med. Devices*, vol. 17, no. 3, pp. 223–233, Mar. 2020.

[3] I. Aprile et al., "Upper limb robotic rehabilitation after stroke: A multicenter, randomized clinical trial," *J. Neurologic Phys. Therapy*, vol. 44, no. 1, pp. 3–14, Jan. 2020.

[4] V. Todorova and A. Blokland, "Mitochondria and synaptic plasticity in the mature and aging nervous system," *Current Neuropharmacology*, vol. 15, no. 1, pp. 166–173, Jan. 2017.

[5] A. G. Guggisberg, P. Koch, F. C. Hummel, and C. M. Buetefisch, "Brain networks and their relevance for stroke rehabilitation," *Clin. Neurophysiol.*, vol. 130, no. 7, pp. 1098–1124, Jul. 2019.

[6] X. Duan et al., "Efficacy of rTMS in treating functional impairment in post-stroke patients: A systematic review and meta-analysis," *Neurol. Sci.*, vol. 45, no. 8, pp. 3887–3899, Aug. 2024.

[7] A. Avenanti, M. Coccia, E. Ladavas, L. Provinciali, and M. G. Ceravolo, "Low-frequency rTMS promotes use-dependent motor plasticity in chronic stroke: A randomized trial," *Neurology*, vol. 78, no. 4, pp. 256–264, Jan. 2012.

[8] J. Lefaucheur et al., "Evidence-based guidelines on the therapeutic use of repetitive transcranial magnetic stimulation (rTMS): An update (2014–2018)," *Clin. Neurophysiol.*, vol. 131, no. 2, pp. 474–528, Feb. 2020.

[9] H.-J. Park and K. Friston, "Structural and functional brain networks: From connections to cognition," *Science*, vol. 342, no. 6158, Nov. 2013, Art. no. 1238411.

[10] M. Corbetta, J. S. Siegel, and G. L. Shulman, "On the low dimensionality of behavioral deficits and alterations of brain network connectivity after focal injury," *Cortex*, vol. 107, pp. 229–237, Oct. 2018.

[11] J. S. Siegel et al., "Re-emergence of modular brain networks in stroke recovery," *Cortex*, vol. 101, pp. 44–59, Apr. 2018.

[12] A. W. L. Xia et al., "Investigating the hemodynamic response to iTBS of the left DLPFC: A concurrent iTBS/fNIRS study," *Brain Stimulation*, vol. 18, no. 2, pp. 235–245, Mar. 2025.

[13] S.-Y. Chen, M.-H. Tsou, K.-Y. Chen, Y.-C. Liu, and M.-T. Lin, "Impact of repetitive transcranial magnetic stimulation on cortical activity: A systematic review and meta-analysis utilizing functional near-infrared spectroscopy evaluation," *J. NeuroEng. Rehabil.*, vol. 21, no. 1, p. 108, Jun. 2024.

[14] J. Riddle et al., "A guide for concurrent TMS-fMRI to investigate functional brain networks," *Frontiers Human Neurosci.*, vol. 16, Dec. 2022, Art. no. 1050605.

[15] E. W. Anderson, G. A. Preston, and C. T. Silva, "Towards development of a circuit based treatment for impaired memory: A multidisciplinary approach," in *Proc. 3rd Int. IEEE/EMBS Conf. Neural Eng.*, May 2007, pp. 302–305:.

[16] Z. Zhang, Z. Li, X. Xiao, Y. Zhao, X.-N. Zuo, and C. Zhu, "Transcranial brain atlas for school-aged children and adolescents," *Brain Stimulation*, vol. 14, no. 4, pp. 895–905, Jul. 2021.

[17] M. Yang, Z. Yang, T. Yuan, W. Feng, and P. Wang, "A systemic review of functional near-infrared spectroscopy for stroke: Current application and future directions," *Frontiers Neurol.*, vol. 10, p. 58, Feb. 2019.

[18] M. Gobbo et al., "Hand passive mobilization performed with robotic assistance: Acute effects on upper limb perfusion and spasticity in stroke survivors," *BioMed Res. Int.*, vol. 2017, pp. 1–6, Sep. 2017.

[19] Z. Tang et al., "The effects of rTMS on motor recovery after stroke: A systematic review of fMRI studies," *Neurological Sci.*, vol. 45, no. 3, pp. 897–909, Mar. 2024.

[20] Z. Keser et al., "Electroencephalogram (EEG) with or without transcranial magnetic stimulation (TMS) as biomarkers for post-stroke recovery: A narrative review," *Frontiers Neurol.*, vol. 13, Feb. 2022, Art. no. 827866.

[21] A. Curtin, S. Tong, J. Sun, J. Wang, B. Onaral, and H. Ayaz, "A systematic review of integrated functional near-infrared spectroscopy (fNIRS) and transcranial magnetic stimulation (TMS) studies," *Frontiers Neurosci.*, vol. 13, p. 84, Feb. 2019.

[22] Y. Liu et al., "Measuring speaker–listener neural coupling with functional near infrared spectroscopy," *Sci. Rep.*, vol. 7, no. 1, p. 43293, Feb. 2017.

[23] S. J. Groiss et al., "Quadri-pulse stimulation induces stimulation frequency dependent cortical hemoglobin concentration changes within the ipsilateral motor cortical network," *Brain Stimulation*, vol. 6, no. 1, pp. 40–48, Jan. 2013.

[24] R. C. Mesquita et al., "Blood flow and oxygenation changes due to low-frequency repetitive transcranial magnetic stimulation of the cerebral cortex," *J. Biomed. Opt.*, vol. 18, no. 6, Jun. 2013, Art. no. 067006.

[25] E. Park, M. J. Kang, A. Lee, W. H. Chang, Y.-I. Shin, and Y.-H. Kim, "Real-time measurement of cerebral blood flow during and after repetitive transcranial magnetic stimulation: A near-infrared spectroscopy study," *Neurosci. Lett.*, vol. 653, pp. 78–83, Jul. 2017.

[26] D. R. de Jesus et al., "Determining optimal rTMS parameters through changes in cortical inhibition," *Clin. Neurophysiol.*, vol. 125, no. 4, pp. 755–762, Apr. 2014.

[27] R. E. Hoffman et al., "Transcranial magnetic stimulation of left temporoparietal cortex and medication-resistant auditory hallucinations," *Arch. Gen. Psychiatry*, vol. 60, no. 1, pp. 49–56, Jan. 2003.

[28] S. Rossi et al., "Safety and recommendations for TMS use in healthy subjects and patient populations, with updates on training, ethical and regulatory issues: Expert guidelines," *Clin. Neurophysiol.*, vol. 132, no. 1, pp. 269–306, Jan. 2020.

[29] F. Nieuwhof et al., "Measuring prefrontal cortical activity during dual task walking in patients with Parkinson's disease: Feasibility of using a new portable fNIRS device," *Pilot Feasibility Stud.*, vol. 2, no. 1, p. 59, Dec. 2016.

[30] F. Awiszus, "On relative frequency estimation of transcranial magnetic stimulation motor threshold," *Clin. Neurophysiol.*, vol. 123, no. 11, pp. 2319–2320, Nov. 2012.

[31] H. Xie et al., "Effects of simultaneous use of m-NMES and language training on brain functional connectivity in stroke patients with aphasia: A randomized controlled clinical trial," *Frontiers Aging Neurosci.*, vol. 14, Sep. 2022, Art. no. 965486.

[32] Q. Tan et al., "Age-related alterations in phase synchronization of oxyhemoglobin concentration changes in prefrontal tissues as measured by near-infrared spectroscopy signals," *Microvascular Res.*, vol. 103, pp. 19–25, Jan. 2016.

[33] H. Xie et al., "Effects of transcranial magnetic stimulation on dynamic functional networks in stroke patients as assessed by functional near-infrared spectroscopy: A randomized controlled clinical trial," *Cerebral Cortex*, vol. 33, no. 24, pp. 11668–11678, Dec. 2023.

[34] L. Xu, B. Wang, G. Xu, W. Wang, Z. Liu, and Z. Li, "Functional connectivity analysis using fNIRS in healthy subjects during prolonged simulated driving," *Neurosci. Lett.*, vol. 640, pp. 21–28, Feb. 2017.

[35] G. Derosière, S. Dalhoumi, S. Perrey, G. Dray, and T. Ward, "Towards a near infrared spectroscopy-based estimation of operator attentional state," *PLoS ONE*, vol. 9, no. 3, Mar. 2014, Art. no. e92045.

[36] F. A. Fishburn, R. S. Ludlum, C. J. Vaidya, and A. V. Medvedev, "Temporal derivative distribution repair (TDDR): A motion correction method for fNIRS," *NeuroImage*, vol. 184, pp. 171–179, Jan. 2019.

[37] K. Zhao, Y. Ji, Y. Li, and T. Li, "Online removal of baseline shift with a polynomial function for hemodynamic monitoring using near-infrared spectroscopy," *Sensors*, vol. 18, no. 1, p. 312, Jan. 2018.

[38] G. Bauernfeind, S. C. Wriessnegger, I. Daly, and G. R. Müller-Putz, "Separating heart and brain: On the reduction of physiological noise from multichannel functional near-infrared spectroscopy (fNIRS) signals," *J. Neural Eng.*, vol. 11, no. 5, Oct. 2014, Art. no. 056010.

[39] P. Raggam, G. Bauernfeind, and S. C. Wriessnegger, "NICA: A novel toolbox for near-infrared spectroscopy calculations and analyses," *Frontiers Neuroinform.*, vol. 14, p. 26, May 2020.

[40] S. Sasai et al., "A NIRS–fMRI study of resting state network," *NeuroImage*, vol. 63, no. 1, pp. 179–193, Oct. 2012.

[41] H. Santosa, M. Jiyoun Hong, S.-P. Kim, and K.-S. Hong, "Noise reduction in functional near-infrared spectroscopy signals by independent component analysis," *Rev. Sci. Instrum.*, vol. 84, no. 7, Jul. 2013, Art. no. 073106.

[42] H. Zhang, Y.-J. Zhang, C.-M. Lu, S.-Y. Ma, Y.-F. Zang, and C.-Z. Zhu, "Functional connectivity as revealed by independent component analysis of resting-state fNIRS measurements," *NeuroImage*, vol. 51, no. 3, pp. 1150–1161, Jul. 2010.

[43] C. Huo et al., "Median nerve electrical stimulation–induced changes in effective connectivity in patients with stroke as assessed with functional near-infrared spectroscopy," *Neurorehabilitation Neural Repair*, vol. 33, no. 12, pp. 1008–1017, Dec. 2019.

[44] Z.-B. Sanders et al., "Self-modulation of motor cortex activity after stroke: A randomized controlled trial," *Brain*, vol. 145, no. 10, pp. 3391–3404, Oct. 2022.
[45] H. Zhang et al., "Exploring the structural plasticity mechanism of corticospinal tract during stroke rehabilitation based automated fiber quantification tractography," *Neurorehabilitation Neural Repair*, vol. 38, no. 6, pp. 425–436, Jun. 2024.
[46] K. J. Friston, "Functional and effective connectivity: A review," *Brain Connectivity*, vol. 1, no. 1, pp. 13–36, Jan. 2011.
[47] A. Bernjak, A. Stefanovska, P. V. E. McClintock, P. J. Owen-Lynch, and P. B. M. Clarkson, "Coherence between fluctuations in blood flow and oxygen saturation," *Fluctuation Noise Lett.*, vol. 11, no. 1, Mar. 2012, Art. no. 1240013.
[48] Q. Han et al., "Phase synchronization analysis of prefrontal tissue oxyhemoglobin oscillations in elderly subjects with cerebral infarction," *Med. Phys.*, vol. 41, no. 10, Oct. 2014, Art. no. 102702.
[49] C. K. Willie, Y.-C. Tzeng, J. A. Fisher, and P. N. Ainslie, "Integrative regulation of human brain blood flow," *J. Physiol.*, vol. 592, no. 5, pp. 841–859, Mar. 2014.
[50] A. R. McFarlan et al., "The plasticitome of cortical interneurons," *Nature Rev. Neurosci.*, vol. 24, no. 2, pp. 80–97, Feb. 2023.
[51] Z. Guo et al., "Distinction of high- and low-frequency repetitive transcranial magnetic stimulation on the functional reorganization of the motor network in stroke patients," *Neural Plasticity*, vol. 2021, pp. 1–11, Jan. 2021.
[52] J. Du et al., "Motor network reorganization after repetitive transcranial magnetic stimulation in early stroke patients: A resting state fMRI study," *Neurorehabilitation Neural Repair*, vol. 36, no. 1, pp. 61–68, Jan. 2022.
[53] L. M. Carey, D. F. Abbott, M. R. Harvey, A. Puce, R. J. Seitz, and G. A. Donnan, "Relationship between touch impairment and brain activation after lesions of subcortical and cortical somatosensory regions," *Neurorehabilitation Neural Repair*, vol. 25, no. 5, pp. 443–457, Jun. 2011.
[54] K. J. Kokotilo, J. J. Eng, M. J. McKeown, and L. A. Boyd, "Greater activation of secondary motor areas is related to less arm use after stroke," *Neurorehabilitation Neural Repair*, vol. 24, no. 1, pp. 78–87, Jan. 2010.
[55] D. E. Nee and M. D'Esposito, "The hierarchical organization of the lateral prefrontal cortex," *Elife*, vol. 5, Mar. 2016, Art. no. e12112.
[56] C. R. Hussar and T. Pasternak, "Common rules guide comparisons of speed and direction of motion in the dorsolateral prefrontal cortex," *J. Neurosci.*, vol. 33, no. 3, pp. 972–986, Jan. 2013.
[57] C. Calautti et al., "The neural substrates of impaired finger tapping regularity after stroke," *NeuroImage*, vol. 50, no. 1, pp. 1–6, Mar. 2010.
[58] M. Pekna, M. Pekny, and M. Nilsson, "Modulation of neural plasticity as a basis for stroke rehabilitation," *Stroke*, vol. 43, no. 10, pp. 2819–2828, Oct. 2012.
[59] F. De Vico Fallani et al., "Interhemispheric connectivity characterizes cortical reorganization in motor-related networks after cerebellar lesions," *Cerebellum*, vol. 16, no. 2, pp. 358–375, Apr. 2017.
[60] Y. He, K. Li, Q. Chen, J. Yin, and D. Bai, "Repetitive transcranial magnetic stimulation on motor recovery for patients with stroke: A PRISMA compliant systematic review and meta-analysis," *Amer. J. Phys. Med. Rehabil.*, vol. 99, no. 2, pp. 99–108, 2020.
[61] W. Y. Hsu, C. H. Cheng, K. K. Liao, I. H. Lee, and Y. Y. Lin, "Effects of repetitive transcranial magnetic stimulation on motor functions in patients with stroke: A meta-analysis," *Stroke*, vol. 43, no. 7, pp. 1849–1857, Jul. 2012.
[62] H. Xiang, J. Sun, X. Tang, K. Zeng, and X. Wu, "The effect and optimal parameters of repetitive transcranial magnetic stimulation on motor recovery in stroke patients: A systematic review and meta-analysis of randomized controlled trials," *Clin. Rehabil.*, vol. 33, no. 5, pp. 847–864, May 2019.
[63] M. Sharbafshaaer, G. Cirillo, F. Esposito, G. Tedeschi, and F. Trojsi, "Harnessing brain plasticity: The therapeutic power of repetitive transcranial magnetic stimulation (rTMS) and theta burst stimulation (TBS) in neurotransmitter modulation, receptor dynamics, and neuroimaging for neurological innovations," *Biomedicines*, vol. 12, no. 11, p. 2506, Nov. 2024.
[64] M. De Michele et al., "Can repetitive transcranial magnetic stimulation (rTMS) promote neurogenesis and axonogenesis in subacute human ischemic stroke?," *Biomedicines*, vol. 12, no. 3, p. 670, Mar. 2024.
[65] F. Scholkmann et al., "A review on continuous wave functional near-infrared spectroscopy and imaging instrumentation and methodology," *NeuroImage*, vol. 85, pp. 6–27, Jan. 2014.
[66] M. D. Pfeifer, F. Scholkmann, and R. Labruyère, "Signal processing in functional near-infrared spectroscopy (fNIRS): Methodological differences lead to different statistical results," *Frontiers Human Neurosci.*, vol. 11, p. 641, Jan. 2018.